

Juha Backman
Nokia Mobile Phones
FIN-00045 Nokia Group, Finland

**Presented at
the 107th Convention
1999 September 24-27
New York**



AES

This preprint has been reproduced from the author's advance manuscript, without editing, corrections or consideration by the Review Board. The AES takes no responsibility for the contents.

Additional preprints may be obtained by sending request and remittance to the Audio Engineering Society, 60 East 42nd St., New York, New York 10165-2520, USA.

All rights reserved. Reproduction of this preprint, or any portion thereof, is not permitted without direct permission from the Journal of the Audio Engineering Society.

AN AUDIO ENGINEERING SOCIETY PREPRINT

A Model of Open-Baffle Loudspeakers

Juha Backman
Nokia Mobile Phones
P.O. Box 100
Nokia Group
Finland

E-mail: juha.backman@nokia.com

0 Abstract

The open-baffle loudspeaker is, although structurally very simple, a challenge for modelling. This paper presents a computationally efficient model for predicting the frequency response and the polar pattern of an open-baffle loudspeaker. The baffle is modelled using time-domain geometrical theory of diffraction, and the conventional driver model is complemented with simple additions to approximate the acoustical asymmetry of the structure.

1 Introduction

Open-baffle loudspeakers are the longest-known¹ and structurally simplest loudspeakers, but they, at the same time, pose considerable theoretical challenges for the modelling. A simple dipole model partially explains some of their features, but such a model is valid only at very low frequencies, and the parameters of the model (e.g. the effective size of the dipole) are difficult to determine. The simple dipole model fails in several respects: it is impossible to take into account asymmetry and other baffle shape effects, the mid-frequency polar pattern is not predicted correctly, etc. Thus taking into account both driver properties and baffle geometry is needed.

The open-baffle speakers do, in addition to being theoretically interesting, have some practical importance. Dipole loudspeakers (and other gradient loudspeakers) provide a constant directivity also at low frequencies. They also excite fewer low-frequency room modes (although the benefit of this is not self-evident) and their acoustical power output is affected by side boundaries much less than the output of omnidirectional speakers².

Despite these advantages the open-baffle speakers are far from being ideal woofers. Their well-known practical problem is their inability to produce adequate low-frequency output. This is a problem particularly with electrostatic and ribbon units (which otherwise are not being discussed within this paper), where the displacement is limited, and there is a trade-off between the displacement and the sensitivity. Larger volume velocities can be achieved by using dynamic woofers, but to maximise their output, a baffle is needed around the driver. The low frequency (dimensions $\ll \lambda$) output of a dipole is proportional to both the volume velocity and the linear dimensions, so doubling the baffle size equals doubling the displacement. This baffle in turn creates

¹ HUNT, FREDERIK V.: *Electroacoustics. The Analysis of Transduction, and Its Historical Background*. Harvard University Press, 1954; reprint Acoustical Society of America, 1982, pp. 86 — 87.

² MORSE, PHILIP M.; INGAARD, K. UNO: *Theoretical Acoustics*, McGraw-Hill, Inc., New York, 1968; reprint Princeton University Press, Princeton, 1986, pp. 372 — 375.

easily problems with mid-frequency response and polar pattern, thus losing the advantages of the open baffle and constraining the usable frequency range.

2 Computational model

2.1 Overview

The open-baffle loudspeaker discussed in this paper consists of a rigid, flat baffle and a circular driver (or multiple drivers) placed at an arbitrary location on the baffle. If only first-order scattering is being studied, the only formal constraint on the baffle shape is that the edge is at least almost convex (i.e. a straight line drawn outwards from the source encounters the edge only at one point; some global concavity is allowed, so far as this condition is fulfilled). When multiple scattering is computed, then the baffle edge has to be convex. Of course in practice only few simple geometries are encountered. The acoustical behaviour of the baffle is described by using time-domain geometrical theory of diffraction, considering both sides separately; important observation that simplifies the analysis is that if the driver is assumed to be symmetrical, then the signal impinging on the edge is identical, but of opposite phase. If simple geometries are considered, then analytical expressions or simple closed-form approximations can be obtained for the impulse responses.

The driver can be regarded to operate almost independently of the acoustical load provided by the baffle, and thus a frequency-domain lumped-component description is appropriate. A significant aspect of the driver function, regarding especially open-baffle applications, is the acoustical asymmetry provided by the chassis, etc. A simple approximation for the asymmetry, which improves the accuracy of predicting mid-frequency polar pattern and response, is to model the chassis as a Helmholtz resonator, which then acts as an acoustical low-pass filter for the rear side of the driver.

For the purposes of creating an efficient model for the open-baffle speaker, several simplifying assumptions need to be made:

- baffle is thin enough as compared to the wavelength in order to be regarded as infinitely thin. In practice this limits the validity of the model to baffles thinner than about $\lambda/4$.
- the radiation from the driver can be approximated by a rigid, circular piston. The frequency responses of the front and rear sides, however, need not be identical (section 2.5), although a symmetrical driver enables further simplification of the model.
- baffle vibration is ignored. This does not affect the accuracy of the diffraction model, but as the baffle area may be much larger than the driver area, the baffle vibration can have a great practical significance.

According to these assumptions, the radiation consists of three components (Figure 1):

- direct sound from the driver
- sound radiated from the front of the driver and scattered from the edges
- sound radiated from the rear of the driver and scattered from the edges

The direct sound can be calculated effectively; the challenges are in determining the near-field sound caused by the driver at the edge and the field scattered from this sound.

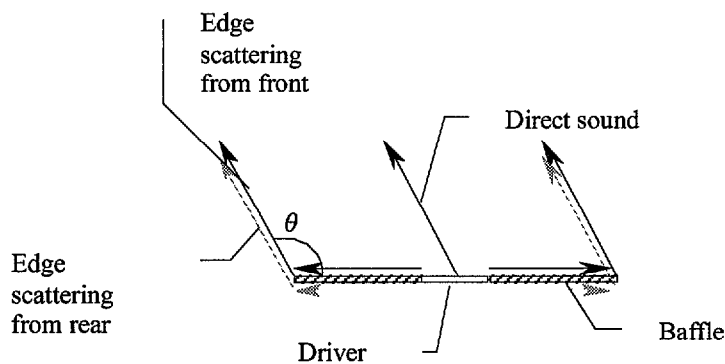


Figure 1. The components of sound radiated by a speaker in a finite open baffle. As indicated below, the scattering strength is determined by the angle θ measured from the front surface of the baffle.

We start by analysing the diffraction of sound emitted by a point source in a baffle. The distance between the edge point

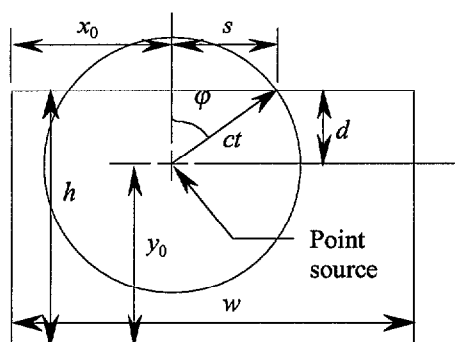


Figure 2. Parameters for describing a point source on a rectangular baffle.

Angle ϕ can be as a function of time in the form

$$\text{Equation 1} \quad \phi = \arccos \frac{d}{ct}$$

The diffracted sound can be represented by directional secondary sources distributed along the edge of the baffle. The strength of the source can be determined by applying the principle of reciprocity and the angular dependence of the sound scattered from an edge point to an angle θ in a plane normal to the edge can be expressed by an equation presented by Vanderkooy³, which for a thin knife-edge wedge simplifies to

$$\text{Equation 2} \quad F(\theta) = \frac{\sin \pi/2}{\cos \pi/2 - \cos \theta/2} = \frac{1}{-\cos \theta/2}$$

³ VANDERKOOY, JOHN: A Simple Theory of Cabinet Edge Diffraction. *JAES*, vol. 39, December 1991, pp. 923 — 933; reprinted in the *AES Anthology Loudspeakers*, vol. 3, pp. 230 — 242.

The shortcoming of this form is that its behaviour near the shadow edge is problematic, but both the illuminated and the shadow regions themselves, especially near the loudspeaker axis, behave rather well.

The sound pressure created at distance r by the radiation from an edge surrounding an open baffle loudspeaker consists of the contributions of the positive and the negative side,

$$\text{Equation 3} \quad p = \frac{\rho dq_+ / dt}{4\pi r} F(\theta) + \frac{\rho dq_- / dt}{4\pi r} F(2\pi - \theta) = \frac{\rho dq_+ / dt}{4\pi r} \frac{4}{-\cos\theta/2} + \frac{\rho dq_- / dt}{4\pi r} \frac{4}{\cos\theta/2}$$

If the driver can be regarded as symmetrical, as usually at low frequencies, then the scattered sound pressure can be simplified to the form

$$\text{Equation 4} \quad p = -\frac{\rho dq / dt}{4\pi r} \frac{2}{\cos\theta/2}$$

When the observation point is not in the normal plane of the edge, then the sound pressure is to be multiplied by a factor $1/\cos\zeta$, where ζ is the angle between the propagation direction and the normal plane.

2.2 Near-field radiation

Although the general near-field radiation problem is notoriously difficult⁴, especially when the calculations are performed in the frequency domain, the problem can be simplified greatly for the purposes of the computation of diffraction. When the field point is constrained to the same plane as the surface of the piston, approximate frequency-domain calculation of the radiation can be done relatively efficiently. In the time domain the situation is even more interesting, since the radiation can be represented by a simple exact expression.

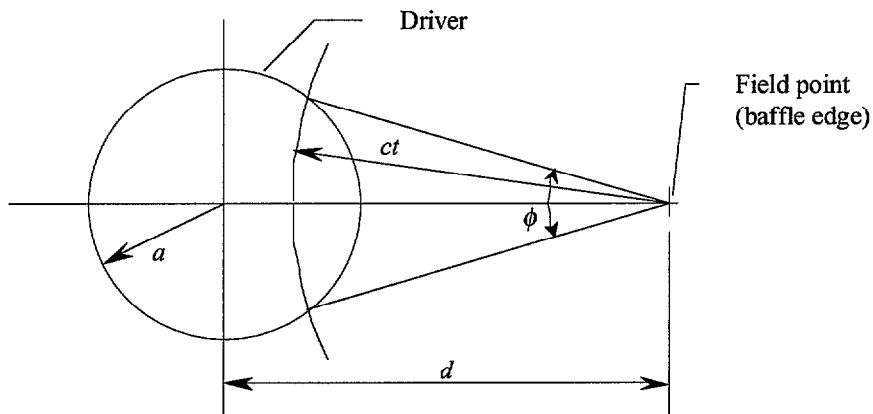


Figure 3. Geometry used in determining the near-field radiation.

The sound pressure dp generated by an area element dA on a piston vibrating with velocity u is

⁴ STENZEL, H.: Über die Berechnung des Schallfeldes von kreisförmigen Membranen in starrer Wand, *Annalen der Physik*, vol. 6, n:o 4, 1949, pp. 303 — 324.

$$\text{Equation 5} \quad dp = \frac{\rho}{4\pi R} \frac{dq}{dt} = \frac{\rho}{4\pi R} \frac{du}{dt} dA,$$

where R is the distance between the field point and the element dA . The distance can be also written as $R = ct$, where t is the propagation time and c the speed of sound.

The surface points corresponding to the sound received at time t form an arc with a radius ct (Figure 3). The area of the surface element is $dA = ctd\phi dt$, which implies that the total sound radiated at time t is

$$\text{Equation 6} \quad p = \int_{-\phi/2}^{\phi/2} \frac{\rho du/dt}{4\pi ct} ctd\phi = \frac{\rho du/dt}{4\pi} \phi.$$

The angle ϕ can be shown to be

$$\text{Equation 7} \quad \phi = \arccos \frac{d^2 + (ct)^2 - a^2}{2ctd},$$

from which the sound pressure can be written as

$$\text{Equation 8} \quad p = \frac{du/dt}{4\pi} \arccos \frac{d^2 + (ct)^2 - a^2}{2ctd}, \quad (d-a)/c < t < (d+a)/c.$$

The volume velocity of the secondary source at the edge per unit angle can be determined from this by multiplying it by ct , which yields

$$\text{Equation 9} \quad q = ct \frac{du/dt}{4\pi} \arccos \frac{d^2 + (ct)^2 - a^2}{2ctd}, \quad (d-a)/c < t < (d+a)/c.$$

The length of the impulse response is independent of the distance of the field point from the driver; it is always $2a/c$. The distance has influence only on the shape of the response.

When the closest point at the edge is reasonably far from the driver (about driver diameter or more), then the impulse response (and spectrum) changes relatively little from one point to another (Figure 4); the largest changes are at high frequencies, where the validity of the model is questionable anyhow. This has one very important implication: under this assumption the diffracted sound can be represented as a convolution of edge diffraction computed using a point source and the driver response. The distance at which the driver impulse response is computed can be chosen to represent an average distance from the edge.

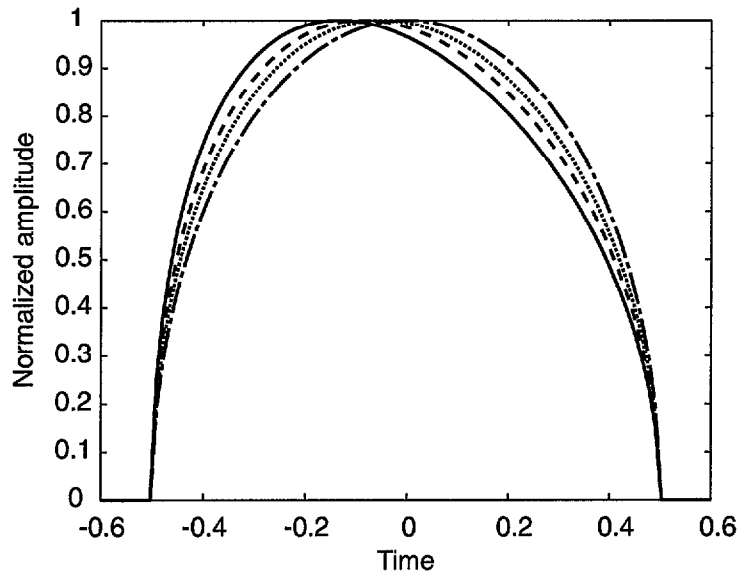


Figure 4. Impulse response at different distance from the source (normalised to the maximum value): solid line: distance = 2 times driver radius, dashed line: distance = 3 times driver radius, dotted line: distance = 5 times driver radius, dash-dot line: distance = 100 times driver radius.

If the model is used calculate the behaviour of a free piston (a totally un baffled speaker), then the radiation model will be numerically difficult (a division by zero) just at the edge. (Analytically, the limiting value can be still shown to be correct.) The numerical difficulties can be circumvented e.g. by assuming a very narrow annular baffle around the driver.

2.3 Multiple scattering

For qualitative description of mid-frequency behaviour, the multiple scattering effects can be ignored. Vanderkooy has demonstrated in his paper⁵, however, that taking multiple scattering is essential for describing low frequencies accurately. As shown later, the effect is even more pronounced for open-baffle speakers. To simplify the analysis the edge is represented again by a discrete set of points. The geometry of baffle has now to be limited to convex shapes, however, since a sound propagating between any arbitrary edge points has to stay inside (or on) the edge.

When calculating multiple scattering the sound propagating on both sides of the baffle has to be taken into account.

⁵ VANDEERKOY, ref. 3.

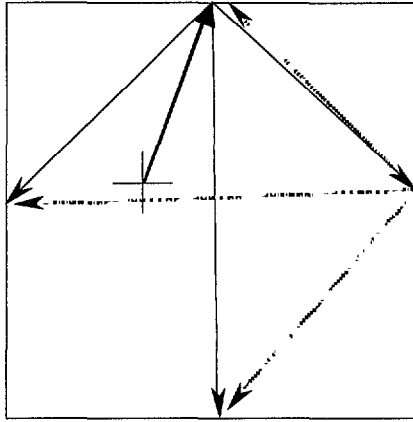


Figure 5. Schematic representation of multiple scattering. Thick solid line = first sound from driver to edge; solid thin line = second-order scattering; dashed line = third-order scattering.

Although the multiple scattering process can be from signal processing point of view regarded to be an IIR filter, representing it as a conventional filter will result in a rather complex and thus memory-consuming network. An alternative way is to represent the signal an edge point as a polynomial of z^{-1} and to use a matrix representation for the multiple scattering:

$$\text{Equation 10} \quad \begin{bmatrix} p_1 \\ p_2 \\ p_3 \\ \vdots \\ p_n \end{bmatrix}_{N+1} = \begin{bmatrix} 0 & a_{2,1} & a_{3,1} & \cdots & a_{n,1} \\ a_{1,2} & 0 & a_{3,2} & & a_{n,2} \\ a_{1,3} & a_{2,3} & 0 & & a_{n,3} \\ \vdots & & & \ddots & \vdots \\ a_{1,n} & a_{2,n} & a_{3,n} & \cdots & 0 \end{bmatrix} \cdot \begin{bmatrix} p_1 \\ p_2 \\ p_3 \\ \vdots \\ p_n \end{bmatrix}_N$$

where N is the order of scattering; $N = 1$ is the first sound arriving from the driver to the edge point.

Each matrix element $a_{i,j}$ consists of a real coefficient representing the scattering amplitude from point i to j and an exponential $z^{-D(i,j)/c}$, where $D(i,j)$ is the distance between the points. In practice the distance (divided by c) can be truncated to the closest integer value to keep the computation simple. If the baffle has straight edges, then the scattering coefficient between any points on the same edge is zero. The multiple scattering matrix is independent of the driver size or position.

The multiplication of the vector consisting of the polynomials by the matrix resembles the convolution of the two; the delays represented matrix, however, are not uniformly spaced or consecutively ordered in each column. Each multiplication corresponds to an operation of delaying and attenuating the sample. The operation could be turned into a proper convolution by arranging each column of the matrix by the power of z^{-1} , merging elements corresponding to the same power and writing the result as an impulse response.

Each scattering naturally lengthens the impulse response. The number of samples added can be estimated simply from the maximum dimension of the baffle. For a 1×1 m² baffle the length of the diagonal is about 1.4 m, which at 100 kHz sampling rate equals about 412 samples. Thus, after 5 scatterings the original impulse response is lengthened only about by 2000 samples.

2.4 Far-field radiation

2.4.1 Radiation from the driver

As far as the direct sound only is concerned, the driver can be regarded to reside in an infinite, flat plane. This approximation can be used even with completely free pistons, since the diffracted part is taken separately into account. There are two ways of representing the far-field direct radiation from a rigid piston: in frequency domain and in time domain. The frequency-domain expression for the sound pressure created by a piston vibrating with a volume velocity q and a frequency f at distance r and angle θ can be represented by the familiar expression⁶

$$\text{Equation 11 } p = -\frac{if\rho q}{r} \frac{2J_1(ka \sin \theta)}{ka \sin \theta}$$

and the time-domain radiation corresponding to a step displacement Δ by the following equation⁷:

$$\text{Equation 12 } p = \begin{cases} 0 & ct < r - a \sin \theta \\ \frac{\rho c^2 \Delta}{2\pi r \sin^2 \theta} \frac{r - ct}{\sqrt{a^2 \sin^2 \theta - (r - ct)^2}} & r - a \sin \theta < ct < r + a \sin \theta \\ 0 & ct > r + a \sin \theta \end{cases}$$

It is easy to see by series expansion that the time-domain expression is an infinite distance limit for the near field expression (Equation 8) presented above. A caveat in using this equation is that it turns into a delta function on-axis; when the analysis is performed in discrete-time domain this is not a problem.

Both the frequency- and time-domain expressions can be used for the direct sound, and the results obtained are equal, but the time-domain expression yields computationally more efficient results.

2.4.2 Radiation from the edges

The delay associated with each edge point can be most conveniently calculated by forming a vector to the observation direction and calculating the projection of a vector connecting a reference point (most conveniently, the centre of the driver) on this vector. The angle to which the sound radiates from the edge segment can be determined in a similar manner, but for that purpose, a normal vector pointing outwards on the plane of the baffle has to be determined.

Especially when the observation angle deviates only little from on-axis, some inaccuracy is caused by rounding the delay to the nearest integer value. In this case the use of fractional delays can be tried⁸. An ideal fractional delay is represented by an offset sinc function, which has two unpleasant properties: infinite extent and non-causality. The former problem can be dealt by suitable windowing and the latter by either a causal approximation (which has some other problems) or by just allowing the impulse response to have some non-causal part. This is not actually very

⁶ MORSE, P. M.: *Vibration and Sound*, 2nd edition, 1948; reprinted by the Acoustical Society of America, 1981, pp. 326 — 328.

⁷ MORSE, ref. 6, pp. 344 — 346.

⁸ LAAKSO, T. I., VALIMÄKI, V., KARJALAINEN, M.; AND LAINE, U. K.: Splitting the unit delay---tools for fractional delay filter design, *IEEE Signal Processing Magazine*, vol. 13, Jan. 1996, no. 1, pp. 30 — 60.

problematic in the actual implementation of the algorithm, since the non-causal part of the energy is small, and since there will be some initial delay from the propagation from the source to the edge point, even windowing away the part causing non-causality in the final result will not have a strong effect on the energy.

After the delays and amplitudes corresponding to each edge point have been determined, then the impulse responses on each edge point are delayed and attenuated by the appropriate amount and added. If fractional delays are used, then this involves explicitly convolving the delay and the impulse response. The use of fractional delays will increase the computation per edge point, but the number of points will be reduced, which reduces the computational load at earlier stages and reduces the amount of memory needed.

The polar pattern can be obtained by computing the frequency response to several angles and tracking the behaviour of a single frequency. An alternative way, which is faster if only a few frequencies are computed, is to go back to the definition of the Fourier transform and compute the inner product of the impulse response to the desired angles with sinusoidals corresponding to the desired frequencies. This yields the spectrum component at that particular frequency. As the magnitude of the transfer function is needed, then for each frequency the multiplication should be done with both a sine and a cosine signal, yielding the imaginary and the real parts.

2.5 Practical drivers

When the frequency range of interest goes well above the fundamental resonance of the driver, the structural asymmetry of a typical transducer must be taken into account. In typical loudspeakers a simple approximation for the structure is to model the volume between the diaphragm and the chassis and the chassis holes as a Helmholtz resonator. The practical problem of this kind of model is that the effective port length becomes difficult to determine computationally, since the distance between the holes and the diaphragm is roughly similar to the dimensions of the holes, and the baffle hole etc. will influence the effective length. The Helmholtz resonator model, however, gives a reasonable qualitative approximation for the asymmetry in the frequency response, although the asymmetry of the radiation pattern (both near-field and far-field) is still ignored.

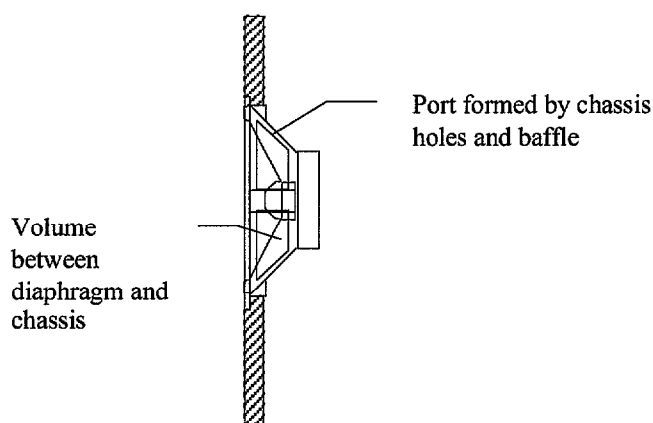


Figure 6. Geometrical parameters describing the Helmholtz resonator approximation for the rear of the driver.

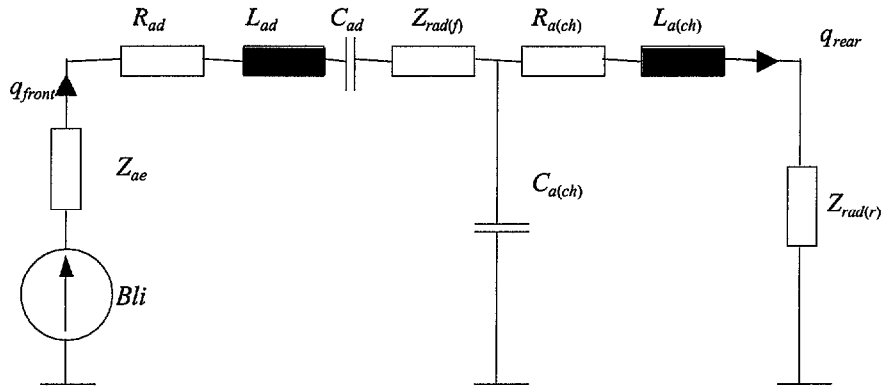


Figure 7. Simple equivalent circuit of a driver, using a Helmholtz resonator to describe the structural asymmetry.

One interesting feature of the simple model described here is that it qualitatively explains why an unbaffled or open-baffle loudspeaker becomes almost omnidirectional at some frequency band in the midrange. Near and above the Helmholtz resonance frequency the driver and chassis port velocities are almost in phase (Figure 8), so the cancellation between front and rear radiation is reduced (and at right angle the sound from both sides is in phase), which typically creates a wider radiation pattern than the driver would have had at the same frequency in an infinite baffle or a sealed enclosure. The optimum condition for omnidirectional radiation (about equal magnitudes, small phase difference) occurs slightly above the Helmholtz resonance frequency.

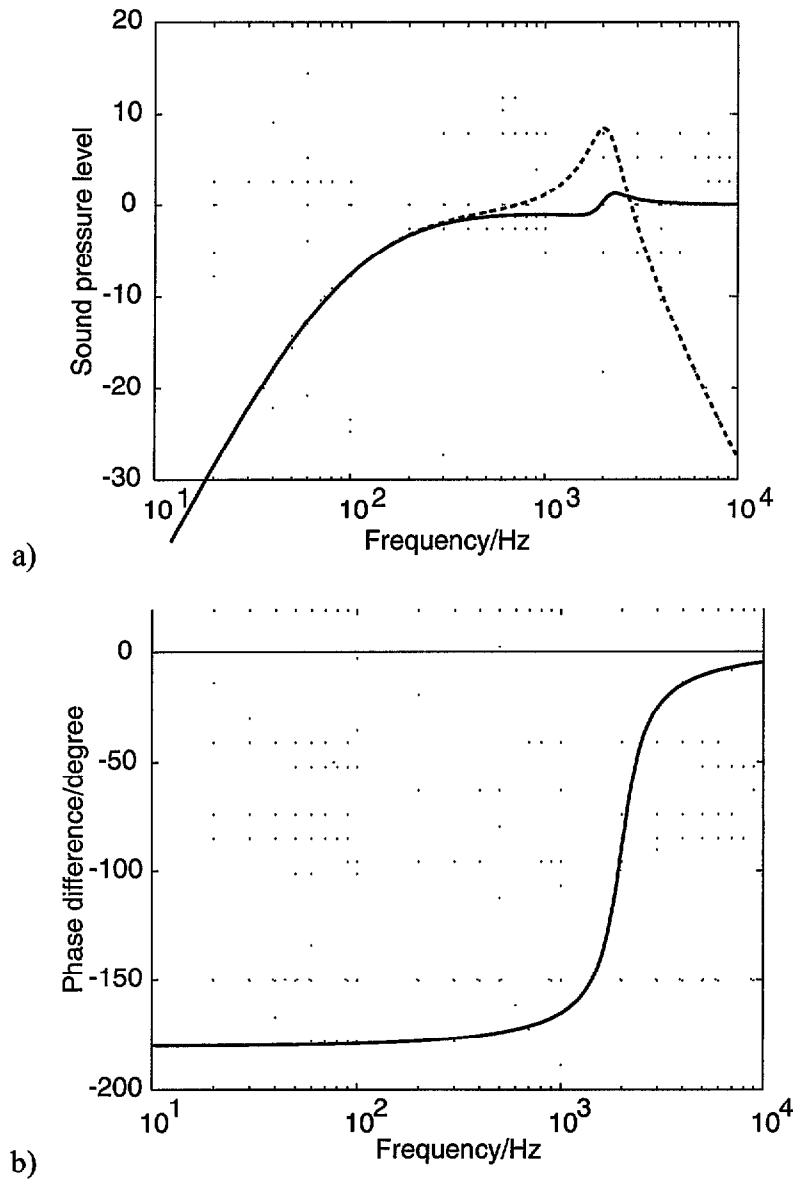


Figure 8. Magnitude (a) of the sound pressure radiated by the front (solid) and rear (dashed) sides a speaker described by the equivalent circuit in Figure 7 and the phase difference between the front and the rear radiation (b). In this example the fundamental resonance is at 100 Hz and the chassis Helmholtz resonance at 2 kHz.

Using this kind of model the acoustical asymmetry can be regarded as a factor independent of the diffraction and the radiation. Thus impulse responses using an idealised source (with a flat response in the far-field on-axis in an infinite baffle) can be used to model the diffraction and the direct sound in the time domain, and the responses can then be transformed into frequency domain to be multiplied by the driver responses and finally to be added (Figure 9).

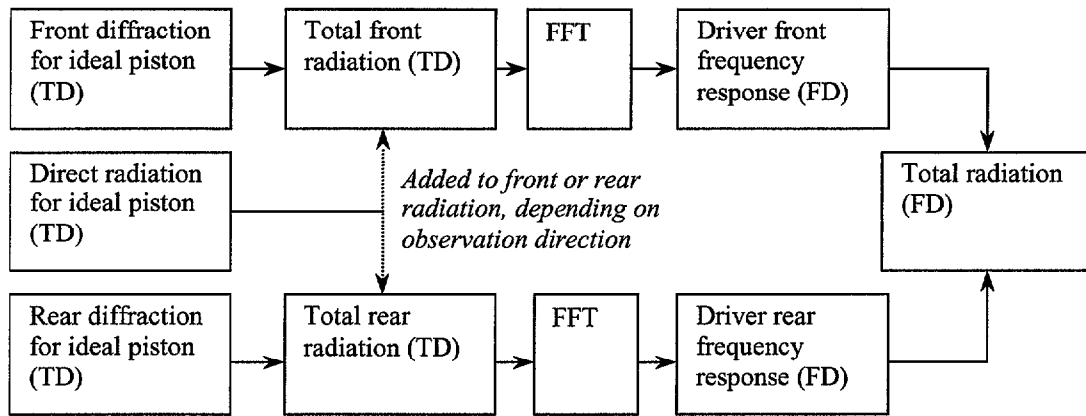


Figure 9. Steps in calculating the total response taking into account the driver properties. TD = time domain calculation, FD = frequency domain calculation.

In practical design work it is possible to mount the driver in a large baffle (significantly larger than the target size of the final design) or a wall, with a large space behind it, and to measure the near-field impulse response in the plane of the baffle at some distance(s) appropriate for the intended final design. The measurements have to be performed for the both sides of the driver using a baffle as thick as the one to be used in the final design, since the baffle thickness affects strongly the asymmetry of the radiation.

The radiation load (for the purposes of this model, mainly attached mass) changes slightly when the driver is in a finite baffle, and thus the resonance is frequency between the free-air and the infinite-baffle values. This can be taken into account by starting with the idealised piston model and calculating the average diffracted sound pressure across the driver on the other side; this yields then a term comparable to the mutual radiation impedance between the driver sides. The correction is small, however.

3 Low-frequency approximation

At very low frequencies the open baffle starts to behave as an ideal dipole, exhibiting the figure-of-eight polar pattern and the additional 6 dB/oct. attenuation as compared to the same driver in an infinite baffle. This low-frequency limit determines the choice of driver parameters (resonance frequency, Q) needed. The radiation of an ideal dipole can be determined from two parameters: volume velocity of the individual monopoles comprising the dipole and their distance. The effective distance is determined from the baffle size and the placement of the driver. As the numerical example in the next section indicates, however, the first-order scattering model yields too low an amplitude at the low frequencies and too high a frequency for the first minimum, which would suggest that the effective distance should be determined from a series expansion describing the multiple scattering.

The effective distance can be assumed to be average distance from the centre of the driver to the edge, calculating the average over the angle measured from the driver (Figure 10). This type of averaging is justified by noting that the sound energy is radiated from the driver to all directions in about the same manner, so the angle averaging equals energy averaging.

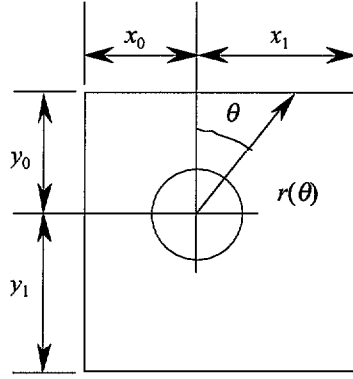


Figure 10. The parameters describing the average distance from the edge.

For a rectangular baffle the distance can be written as

$$\text{Equation 13 } r(\theta) = \frac{r_0}{\cos\theta},$$

where r_0 is the distance from the edge under study and θ the angle calculated for that particular edge. If the edge is delimited by angles θ_{\min} and θ_{\max} , then the average distance is

$$\begin{aligned} \text{Equation 14 } r_{ave} &= \frac{1}{\theta_{\max} - \theta_{\min}} \int_{\theta_{\min}}^{\theta_{\max}} \frac{r_0}{\cos\theta} d\theta = \frac{1}{\theta_{\max} - \theta_{\min}} \left. \ln \sqrt{\frac{1 + \sin\theta}{1 - \sin\theta}} \right|_{\theta_{\min}}^{\theta_{\max}} \\ &= \frac{1}{\theta_{\max} - \theta_{\min}} \ln \left(\frac{\sqrt{1 + \sin\theta_{\max}}}{\sqrt{1 - \sin\theta_{\max}}} / \frac{\sqrt{1 + \sin\theta_{\min}}}{\sqrt{1 - \sin\theta_{\min}}} \right) \end{aligned}$$

Taking the uppermost edge as an example, the minimum and maximum angles for an edge can be defined from the geometry of the baffle as

$$\begin{aligned} \text{Equation 15 } \theta_{\min} &= -\arcsin \frac{x_0}{x_1^2 + y_0^2}, \\ \theta_{\max} &= \arcsin \frac{x_1}{x_1^2 + y_1^2}, \end{aligned}$$

from which the average distance for this particular edge can be written as

$$\text{Equation 16 } r_{ave, 1} = \frac{1}{\arcsin \frac{x_1}{x_1^2 + y_0^2} + \arcsin \frac{x_0}{x_0^2 + y_0^2}} \ln \left(\frac{\sqrt{1 + \frac{x_1}{x_1^2 + y_0^2}} \sqrt{1 + \frac{x_0}{x_0^2 + y_0^2}}}{\sqrt{1 - \frac{x_1}{x_1^2 + y_0^2}} \sqrt{1 - \frac{x_0}{x_0^2 + y_0^2}}} \right).$$

Repeating this for other edges yields the total average distance, from which can be computed the estimate for the on-axis sound pressure at distance r

$$\text{Equation 17 } p = \frac{i\rho\omega^2 q r_{ave}}{4\pi r c}$$

where q is the volume velocity corresponding to one side of the driver.

The frequency of the first minimum (on-axis) is according to this model

Equation 18
$$f_{\min} = \frac{c}{r_{ave}}$$

4 Numerical example

The results obtained by the method are illustrated by the results obtained from the baffle illustrated below (Figure 11).

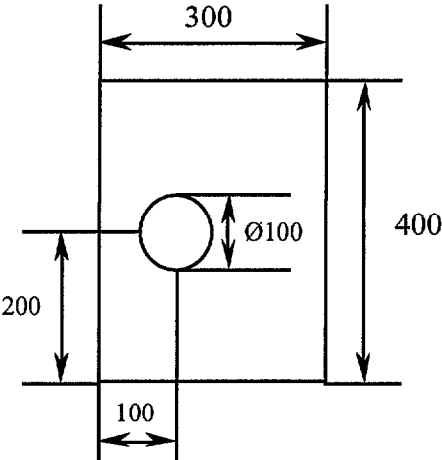


Figure 11. The baffle used in the examples (all dimensions in mm).

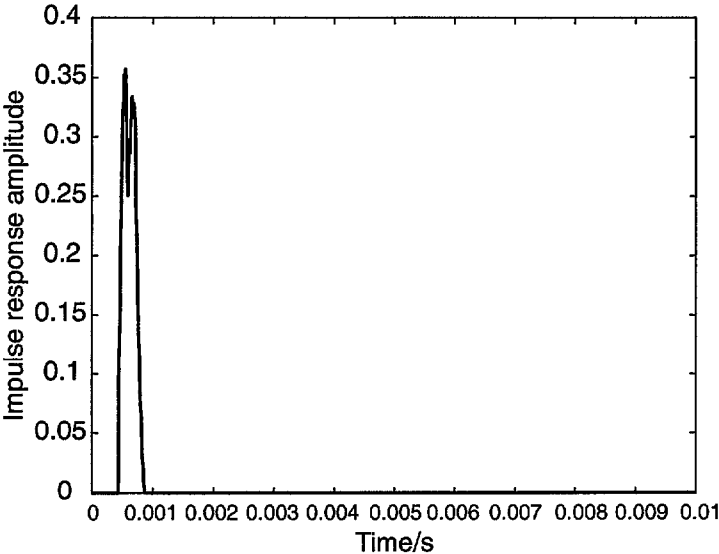


Figure 12. Impulse response of the first-order scattered sound.

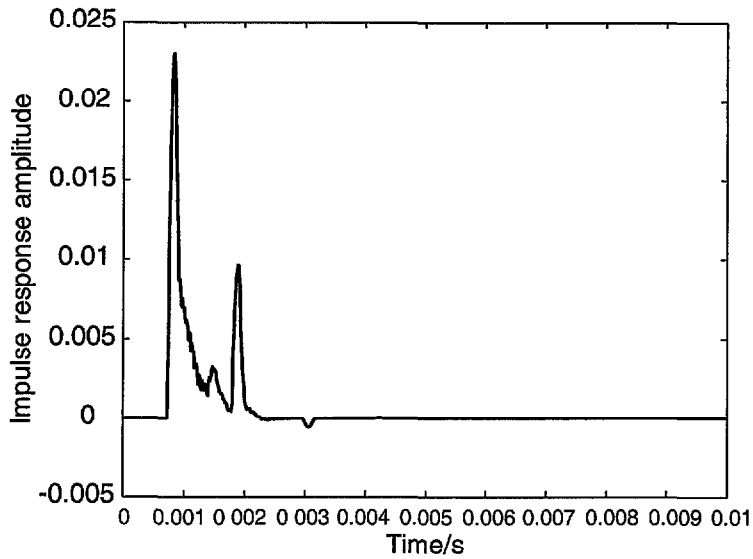


Figure 13. Impulse response of the scattered sound, taking into account the scattering up to 5th order.

An interesting feature is that the average decay characteristics are almost perfectly exponential (Figure 14).

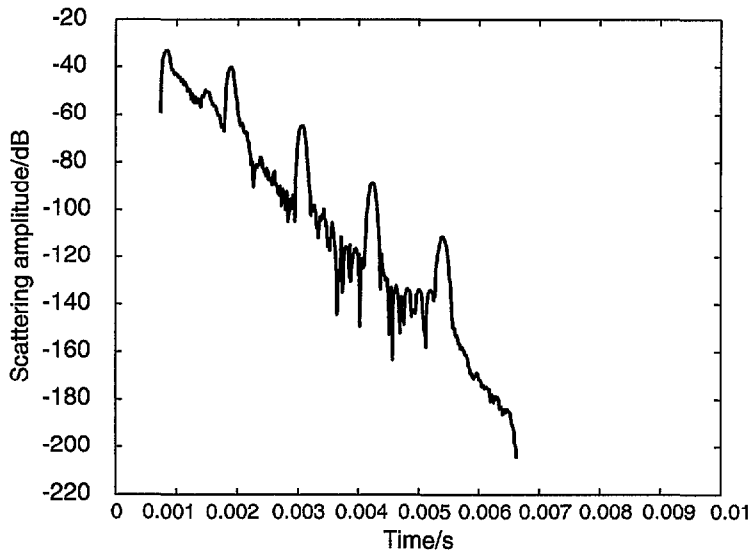


Figure 14. Decay characteristics of the scattered sound, plotted on a logarithmic scale.

The importance of multiple scattering is clearly illustrated from the frequency responses calculated using the impulse responses shown above. (The edge impulse response is subtracted from the direct sound, if the sign of the diffracted sound is chosen as illustrated; in a physical system the sign of the diffracted sound in the illuminated region is opposite to the direct sound, and in the shadow region the same.) The response predicted using only single diffraction indicates too much low-frequency attenuation and too large local minima and maxima in the response.

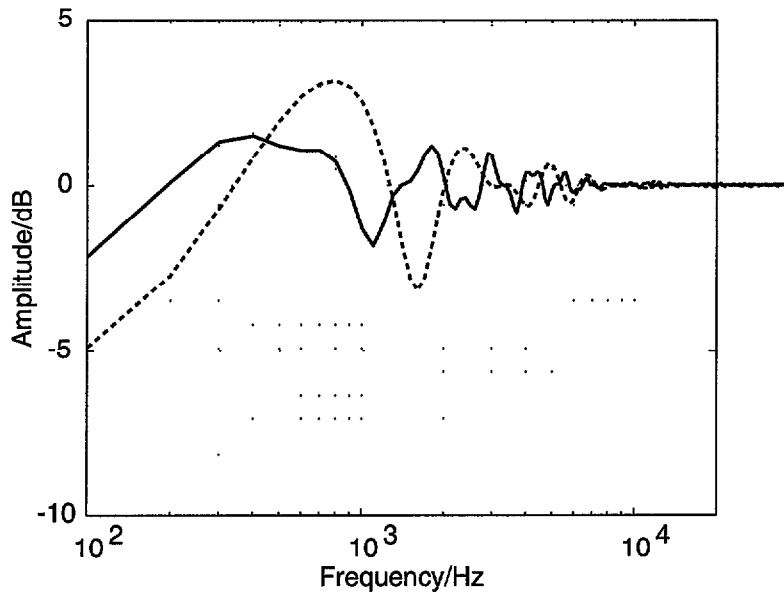


Figure 15. Frequency response corresponding to 1st-order scattering (dashed line) and 5th-order scattering (solid line).

5 Conclusions

The method presented here enables a fast calculation of the characteristics of an unbaffled loudspeaker. The model is quite usable for calculating the frequency response up to angles approaching the shadow boundary, but is problematic in predicting the behaviour at the plane of the baffle. The numerical simulations shown indicate clearly that multiple scattering has to be taken into account.